PROCEEDINGS OF SPIE

SPIEDigitalLibrary.org/conference-proceedings-of-spie

Wavefront preserving optics for diffraction-limited storage rings and free-electron lasers

Daniele Cocco, Daniele Spiga

Daniele Cocco, Daniele Spiga, "Wavefront preserving optics for diffraction-limited storage rings and free-electron lasers," Proc. SPIE 11111, X-Ray Lasers and Coherent X-Ray Sources: Development and Applications XIII, 111110G (11 September 2019); doi: 10.1117/12.2531862

SPIE.

Event: SPIE Optical Engineering + Applications, 2019, San Diego, California, United States

Wavefront preserving optics for diffraction-limited storage rings and free-electron lasers

Daniele Cocco*[a,b], Daniele Spiga[b]
[a] Lawrence Berkeley National Laboratory, Berkeley, CA USA 94720;
[b] SLAC National Accelerator Laboratory, 2575 Sand Hill Rd. Menlo Park, CA, 94025

*dcocco@lbl.gov; phone 1 510-486-7110; https://als.lbl.gov/people/daniele-cocco/

ABSTRACT

With the advent of Diffraction Limited Storage Rings (DLSR) and the Free Electron Lasers (FEL), the challenge for optical designers is to achieve diffraction-limited spot in the experimental chamber preserving the wavefront. This improvement permits working out of focus with almost uniform beam. To reach this level of quality on the beam, one should go behind the Marechal Criterion, stating that a Strehl Ratio (SR, e.g. the ratio between the intensity on the spot for a perfect optical system and the actual one) of 0.8 is a synonymous of a well performing optic system. In reality, a Strehl ratio in excess of 0.95 is needed for wavefront preserving purposes. This corresponds having long mirrors polished at a precision of better than 1 nm rms. With the initial upgrade of the photon transport system of LCLS we demonstrated that it is possible to have an "almost" perfect beam out of focus putting proper attention to all the details and, aiming for a SR of 0.97. But, besides the high precision shape error, some other details shall be considered. For instance, how many beam sigma one should consider for the specifying his mirror and, also, does the slope errors play any role in the quality of the beam out of focus? Moreover, with the advent of SXR DLSRs, it's important to understand the requirements for the gratings, behind the shape and slope errors, e.g. on the precision of the groove placement. Also, in this case, the Strehl Ratio is a good way for assessing this problem.

Keywords: Diffraction limited optics, Wavefront preservation, Marechal Criterion, Grating groove precision, Strehl Ratio.

1. INTRODUCTION

The pioneering early days of synchrotron radiation, with rings like Tantalus, SURF, ADONE, DESY and others, were benefit of new sources, with unprecedent capabilities, new techniques, new users and almost no competition. With the second-generation storage rings, several facilities were built around the world, following the initial interests on the 1st generation sources. SRS, SSRL, Aladdin, NSLS, LURE, SRC, MAX, Bessy, Photon Factory among the many, showed an increase number of users, with increased demands and ideas. The requests of higher performance and beam quality, led the various laboratory to start implementing X-ray optics groups, not only to face the increasing user demands but, also, if not mostly, to face the competition of the other facilities. This has been, until recently, one of the periods in time that have seen the most rapid and drastic improve in X-ray optics with, for instance, the development of simulation software [1], metrology [2,3] and, for instance, Soft X-ray (SXR) monochromators [4-11]. In the latter case, it is particularly impressive, if compared with the very few novel designs developed in the following two decades [12-15].

To do not forget are the various improvement, made in the 90s and early 2000, to the quality of the optics, metrology, crystal, gratings, zone plate and others. But, a novel approach to optics and optical design, didn't happen, until new kind of facilities (the Free Electron Lasers) came on line and battled for users and funds. As an example, both FLASH (the first UV FEL) and LCLS (the first X-ray FEL) started operation without a real optics group. Nonetheless, pioneering work made in both, FLASH and LCLS [16-19], has to be recognized as it paved the way to are to the future boost in optics development that, mostly, happen with the advent of Fermi@Elettra [20], XFel, SACLA, Swiss-FEL and others. New challenges came along, related to the high peak photon pulse energy and short pulse duration. In the meantime, thanks to the development made at the Osaka University [21], diffraction limited optics became available from JTEC Corp [22]. Thanks to these mirrors, diffraction limited nano-scale spots [23] or almost perfect beam out of focus [24] were made possible.

X-Ray Lasers and Coherent X-Ray Sources: Development and Applications XIII, edited by Annie Klisnick, Carmen S. Menoni, Proc. of SPIE Vol. 11111, 111110G · © 2019 SPIE
CCC code: 0277-786X/19/$21 · doi: 10.1117/12.2531862

As explained in [25], to be able to work out of focus, a Strehl Ratio above 0.95 is necessary. The Strehl Ratio is the ratio between the measured (or simulated) intensity in focus and the ideal one [26]. A simple formula to calculate the Strehl Ratio (SR) is:

$$\text{Strehl Ratio} \approx e^{-(2\pi\varphi)^2} \approx 1-(2\pi\varphi)^2 \tag{1}$$

where φ is the phase shift introduced by δh, the rms shape deviation from the ideal mirror profile. It can be calculated as:

$$\varphi = \frac{2\delta h \sin\vartheta}{\lambda} \tag{2}$$

and θ is the grazing angle of incidence. From the previous two equations, one can derive the required shape error for a given Strehl Ratio as:

$$\delta h = \lambda \frac{\sqrt{1-Strehl \quad Ratio}}{4\pi \sin\vartheta} \tag{3}$$

As an example, for the LCLS Hard X-ray Mirror upgrade, where the angle of incidence was 1.35 mrad, and the wavelength as low as 0.1 nm, a δh < 0.5 nm rms was required for aiming at a SR above 0.95. This is, of course, a very challenging goal to achieve. Indeed, mirrors with such surface quality exist and yielded a nearly-perfect beam out of focus at LCLS [see figure 1 left]. Beside the need of a SR in excess of 0.95, also the effect of the slope errors has been revisited in the recent years. As pointed out by Pardini and co-authors [27], if the beam is fully coherent, the only things that matter, in specifying the mirrors, are the shape errors. The slope errors don't play any important role in the quality and dimension of the spot in focus.

Even if this statement is true, in this article we want to make a further step and show how, if someone is planning to work out of focus, the slope errors are, actually, important. Another important aspect, in specifying the optics, is on which mirror aperture (i.e. illuminated length) the shape errors have to be considered when using equation 2. This will be also described in this article. Finally, the Strehl Ratio will be used to calculate the effect of groove irregularities in diffraction gratings. A formula to estimate the groove ruling tolerances is also given.

2. OUT-OF-FOCUS BEAM QUALITY: EFFECT OF THE SLOPE ERRORS AND OF THE BEAM FOOTPRINT

In [27] it was clearly (and correctly) stated that the mirror slope errors do not play any major role in decreasing the quality of the focus of a diffraction limited spot. Of course, the quality of the focused spot is the most common and important situation for an experiment. However, an increasing number of experiments involve out of focus geometries. This may be due, for instance, to prevent the sample from being damaged by the intense radiation, or to uniformly illuminating a sample, like in Photo Electron Emission Microscopy. Since working out of focus is a common practice at LCLS, the Hard X-ray mirrors and the holders that have been designed, procured and installed recently are aimed to have a SR in excess of 0.95. Two of the procured flat mirrors, produced by JTEC, have shape errors as shown in fig.1 right. These two mirrors were the first two in the HXR beamline and have shape errors of 0.53 and 0.49 nm rms. The slope errors are below 150 nrad rms in the first case and below 100 nrad in the other. As a result, an almost perfect beam out of focus has been achieved [figure 1 left].

Even if the spot shown in figure 1 left is very good, and is almost perfect for the purpose of the experiments, some unwanted striations in the intensity profile can be detected. Looking at the presence of high frequency components in the

shape error of the mirror profile, one may associate this high frequency error to the high frequency wavefront distortion in the spot. To verify this first impression, let us consider a 0.5 nm rms shape error mirror, like the one of the existing mirrors but, with higher slope errors. A simulation, using the program WISE [28] on OASYS [29,30] has been made using the existing mirror profile. The result is shown in figure 2, lower left panel.

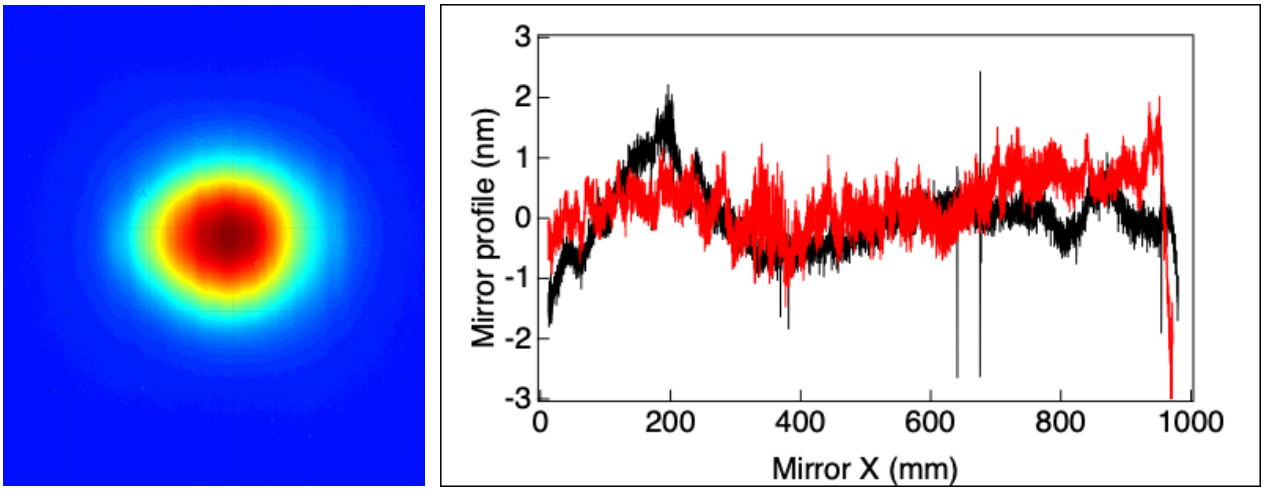

Figure 1: LEFT: Unfocused measured beam profile in the HXR beamline of LCLS after two mirrors at 9 keV photon energy. RIGHT: shape profile of the two mirrors delivering the beam to the screen where the image in the left panel has been recorded. The rms shape errors of the two mirrors are 0.53 and 0.49 nm rms.

We can now repeat the simulation, after replacing the red curve of figure 1 with the red curve shown in figure 2 top panel. This is still a 0.5 nm rms shape error, containing high frequency components. The overall slope errors go up to above 300 nrad rms. The effect of this high frequency components is shown in figure 2 lower right panel. It is evident that this second beam profile is not as good as the first one and highly distorted (even if still on good enough quality to be used). This simple comparison shows how important is to properly specify and control the mirror during production.

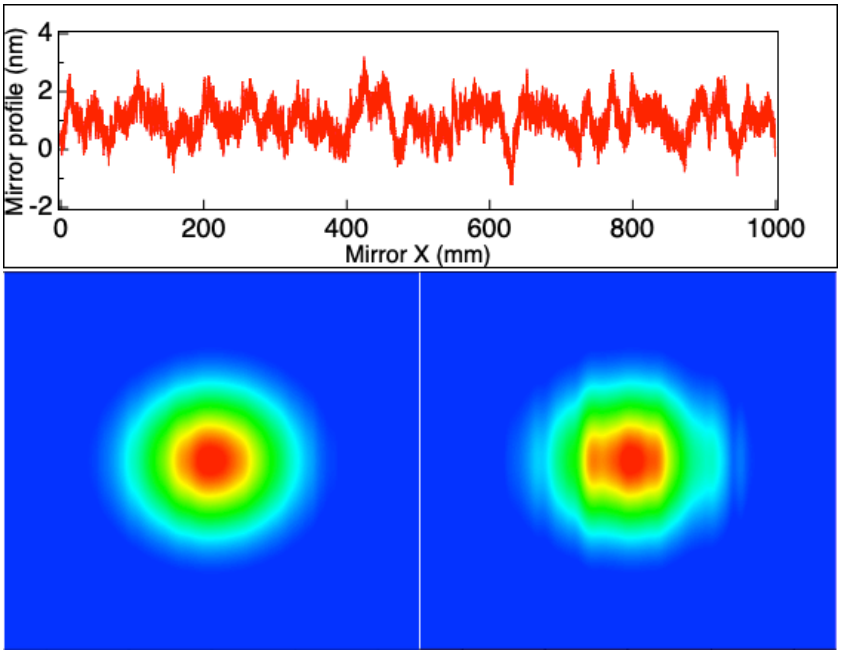

Figure 2: Upper panel: artificially generated mirror profile with 0.5 nm rms and 300 nrad rms slope errors. Lower panel: Comparison of the simulated beam using the measured profile of the mirror installed in the LCLS HXR line (left) and the case in which, one of the two mirrors has the profile shown in the upper panel of this figure. The effect of the higher slope error is evident.

If one thinks that usually the vendor doesn't produce mirrors with high frequency components, he/she is probably mistaken. Usually vendors do not measure mirrors with high spatial frequency, and neither do most of the metrology laboratories at the Synchrotron or FEL facilities. But, the effect of not controlling the high spatial frequencies and the slope errors, may highly impacting the quality of the beam. We note that, the calculated Strehl ratio, in both cases, is of the order of 0.97, but, this does not describe properly the result. Therefore, the SR, out of focus, is not enough to predict the behavior of a give mirror.

It is widely accepted that the footprint of the beam on the mirror plays an important role in determining the final quality of the image. From the aberration theory, described, for instance, in [31], the footprint is directly linked to the amount of aberration in the spot. But, in calculating the Strehl Ratio, a different criterion shall be used, rather than the use of the 1 FWHM (Full Width at Half Maximum). Goldberg and Yatchuck in [32] have described a method for optimizing (maximizing) the Strehl Ratio for a focusing optics. Here, we simply want to give a general rule for defining on which mirror aperture the shape errors have to be considered for calculating the SR.

Let's consider four different mirror profile, as shown in figure 3. The blue one can be similar to what is expected in the case of a thermal bump, the red one is a quite common shape profile, the green is quite unusual and the black is created to highlight the change of shape error with the aperture. In figure 3 right, the rms shape errors are calculated as a function of the mirror aperture. The colors on the right panel match the colors on the left one. Let's now consider three different beams with same wavelength (1 nm or 1240 eV) but different beam divergence. In this simulation, the 1 m long mirror is positioned100 m from a diffraction limited source, focusing 2 m downstream. The footprint of the 3 beams on the mirror, with an angle of incidence of 0.5º, are 143, 187 and 269 mm FWHM.

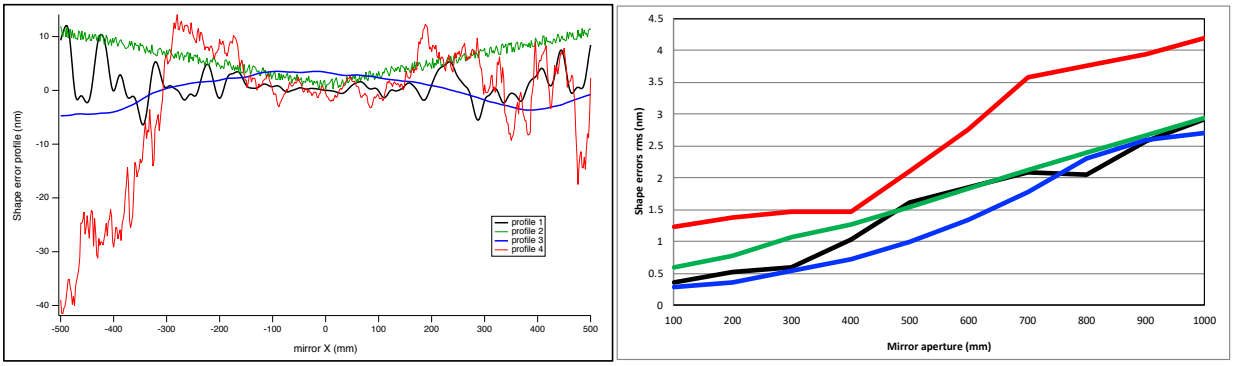

Figure 3: Left: Four different shape error profile for a 1 m long mirror and Right: the calculated rms shape error vs the mirror aperture.

The focused beam for the four slope profiles and for the 3 divergences are shown in figure 4. Each different of the 3 panels showing the cross section of the beam in focus, represent a different beam divergence (e.g. footprint). From these simulations, one can directly "measure" the Strehl Ratio. This is reported in the lower right box of figure 4. In this box, different colors represent different shape error curves. Same color code as in figure 3. The measured SR is reported with dots (squares or triangles) for two different footprints, the squares are located at an aperture of 1 FWHM and the triangle at an aperture of 2 FWHM.

From figure 3 left and from equations 1 and 2, one can calculate the SR as a function of the mirror aperture, for the various shape profiles. It is quite evident that the SR calculated over 2 FWHM is the one matching the "measured" SR after simulations. Therefore, without the need of performing simulations, one can simply calculate the rms shape errors on the mirror over 2 FWHM and derive from there the SR. Note that this is true also in the case of thermal bumps, similar to the blue curve in figure 3. But, if a bender is present, one should remove, at least, the spherical part from the residual shape error when the SR is calculated.

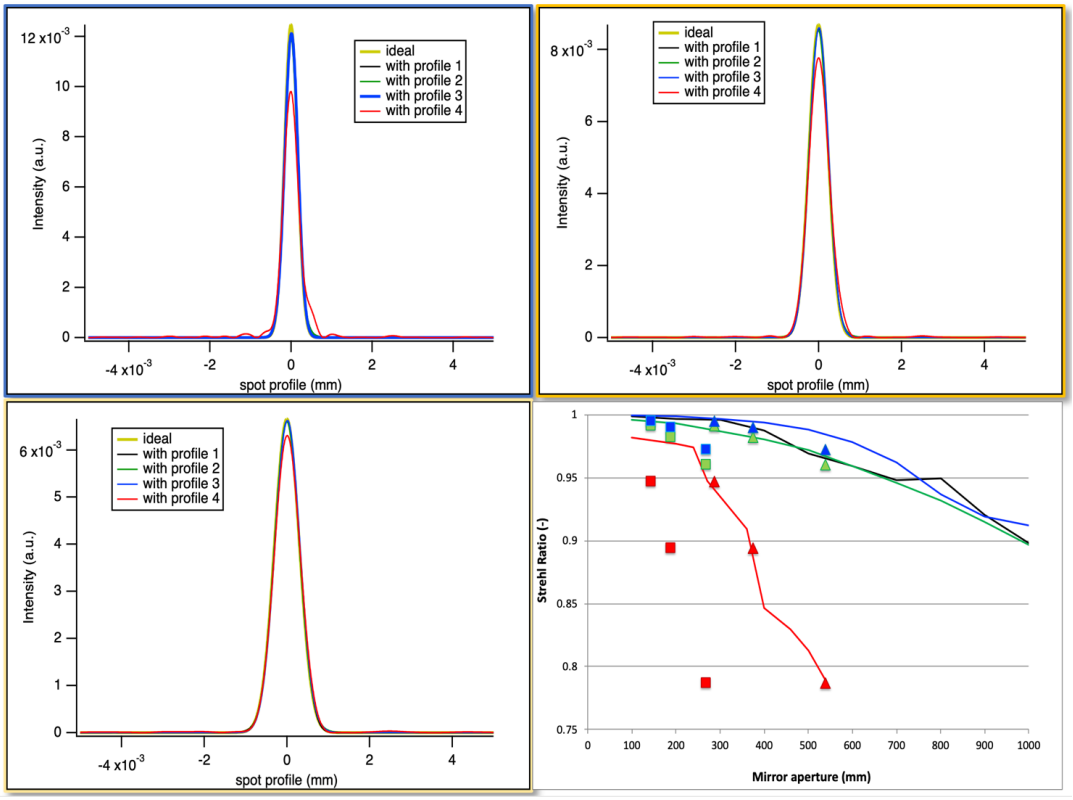

Figure 4: Spot profile (upper 2 panels and lower left panel) for three different beam divergences. Each of these 3 panels shows the focus profile for an ideal mirror (gold) and for the four shape errors shown in figure 3. The lower right panel represent the calculated SR (full lines) from figure 3 right and the measured from the other three panels (dots). The measured one is reported for a mirror aperture of 1 (squares) and 2 (triangles) FWHM.

3. THE STREHL RATIO FOR DIFFRACTION GRATINGS

Diffraction gratings have been used extensively since several decades. Holographically recorded and mechanical ruled gratings provide efficient tools for investigation ranging from astronomy to nano-scale microscopy and from deep infrared to tender X-ray. For the gratings produced for Soft X-ray application [33], few techniques for measuring the precision of the groove placing have been developed. In the late 90ies, Irick and McKinney suggested using the long trace profiler (LTP) for measuring the gratings in Littrow condition [34]. The technique has been further optimized and extended to Variable Line Spacing (VLS) Grating [35]. A Fizeau 2D interferometer has also been used to test the groove placing error. While the idea is quite old, only recently it has been published by Gleason at al. [36]. Of course, the capability to characterize a grating enables one to affordably predict the focused spot shape/size, consequently, the resolving power. But, before doing it, one needs to specify the grating and provide this requirement to the vendor. At this regard, we hereafter provide a relatively easy way to estimate the precision needed for a particular system.

The idea is to use the Strehl Ratio as shown in equation 1. As a reminder, that particular equation is valid for SR close to 1. And this is the target of our discussion here, since we want to have gratings with sufficient quality to preserve the resolution as much as possible. Equation 2 defines the phase error introduce to the reflected beam due to mirror defect. We now need to do the same for gratings: we calculate the phase error on the beam diffracted by a grating due to absolute groove misplacement, e.g., the ability of positioning the groove in the correct location over the entire length of the grating.

To calculate it, let us represent the field diffracted by the grating, at the diffraction peak as follows:

$$E_G = \sum_{k=1}^{N} E_D e^{-\frac{2\pi i}{\lambda}(\cos\alpha - \cos\beta)x_k} \tag{4}$$

where E_D is the diffracted field by a single facet in the grating profile, α is the off-surface incidence angle, β the off-surface diffraction angle, and x_k is the coordinate of the center of the k-th facet. The position of the facet can be written as $x_k = kd + y_k$, where d is the grating step (slowly variable in the case of a VLS) and y_k is the deviation from the nominal groove location. As we assume to be at the 1st diffraction peak, the grating formula is exactly fulfilled: $\cos\alpha - \cos\beta = \lambda/d$, therefore we can rewrite the SR as

$$\mathrm{SR} = \left| \frac{\sum_{k=1}^{N} E_D e^{-\frac{2\pi i}{d} y_k}}{\sum_{k=1}^{N} E_D e^{-2\pi i k}} \right|^2 \tag{5}$$

Neglecting changes in the obliquity factor throughout the grating length, E_D is a constant and, dubbing with L the grating length, we rewrite the SR as

$$\mathrm{SR} = \frac{1}{L^2} \left| \sum_{k=1}^{N} e^{-\frac{2\pi i}{d} y_k} d \right|^2 \tag{6}$$

if $d \ll L$, we can approximate the sum with an integral and write

$$\mathrm{SR} = \left| \int_0^L e^{-\frac{2\pi i}{d} y_x} \frac{\mathrm{d}x}{L} \right|^2 \tag{7}$$

in order to compute this integral, we replace the uniform distribution of groove position errors, $\mathrm{d}x/L$ with a Gaussian probability distribution with rms δ, and we sum over y instead of x:

$$\mathrm{SR} = \left| \frac{1}{\delta\sqrt{2\pi}} \int_{-\infty}^{+\infty} e^{-\frac{2\pi i}{d} y} e^{-\frac{y^2}{2\delta^2}} \mathrm{d}y \right|^2 \tag{8}$$

and we obtain, after some handling:

$$\mathrm{SR} = \frac{1}{2\pi\delta^2} e^{-\left(\frac{2\pi\delta}{d}\right)^2} \left| \int_{-\infty}^{+\infty} e^{-\left(\frac{y}{\delta\sqrt{2}} + \frac{\delta\pi i\sqrt{2}}{d}\right)^2} \mathrm{d}y \right|^2 \tag{9}$$

and since the Gaussian integral in || brackets clearly amounts to $\delta(2\pi)^{1/2}$, the SR reduces to:

$$\mathrm{SR} = e^{-\left[\frac{2\pi\delta}{\lambda}(\cos\alpha - \cos\beta)\right]^2} \tag{10}$$

Therefore, the phase error induced by the groove density error is:

$$\varphi = \frac{\delta}{\lambda}(\cos\alpha - \cos\beta) \tag{11}$$

Equation 11, in conjunction with equation 1 (or equation 10) can be used to calculate the SR of a diffraction grating.

To validate this statement and to give an idea of the precision needed in manufacturing a grating for a fully coherent beam, let's consider the monochromator designed for the LCLS upgrade project [37]. This is based on four gratings, one for low resolution and 3 for high resolution. Let's focus on a grating that has been received and measured.

The grating has 300 l/mm and works with a Cf factor of 3.2. The distance grating exit slit is 19.6 m and the target resolving power is expected to be in excess of 50,000. Some simulations, using WISE, have been made for this grating and are shown in figure 5. The curves reported there, are for the 500 eV case, and represent the simulated energy distribution after the exit slit, in the case of an ideal grating (red curve) and for gratings with increasing error in the groove placement (left panel). As an example, three of the curves, representing the deviation between the ideal location of a given groove and the actual one used for the simulation, are shown in figure 6.

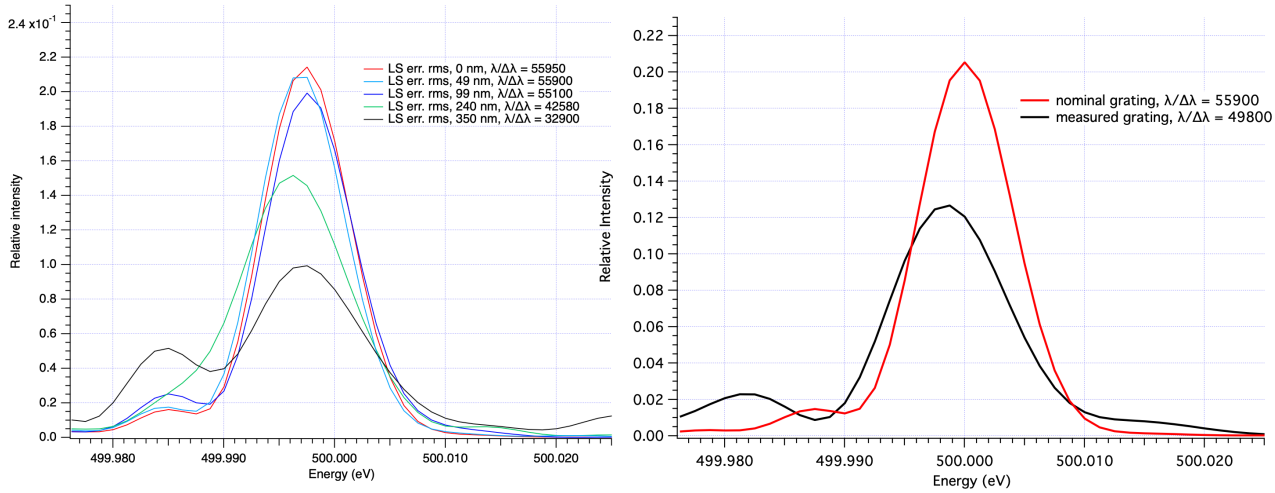

Figure 5: Simulated energy distribution after a 5 μm exit slit for the 300 l/mm grating. The simulation is performed considering an ideal grating (red curves) or with increasing rms pitch error on the grooves. RIGHT: Simulation of the expected performance of the same grating at the same energy, using the measured groove placing error.

The reduction in resolving power is evident and is reported in the figure legend and in table 1. The same simulation has been made by using the measured groove placing error. The measured placing error is shown in figure 7. The measurement has been made by following the procedure in [35] from which one obtains the local groove density and, consequently the local groove density variation. From this value, the local d-spacing error (or groove pitch error) is calculated. Integrating this value over the grating, one obtains the required groove placing error, e.g., the distance from the ideal location of a groove and the actual one.

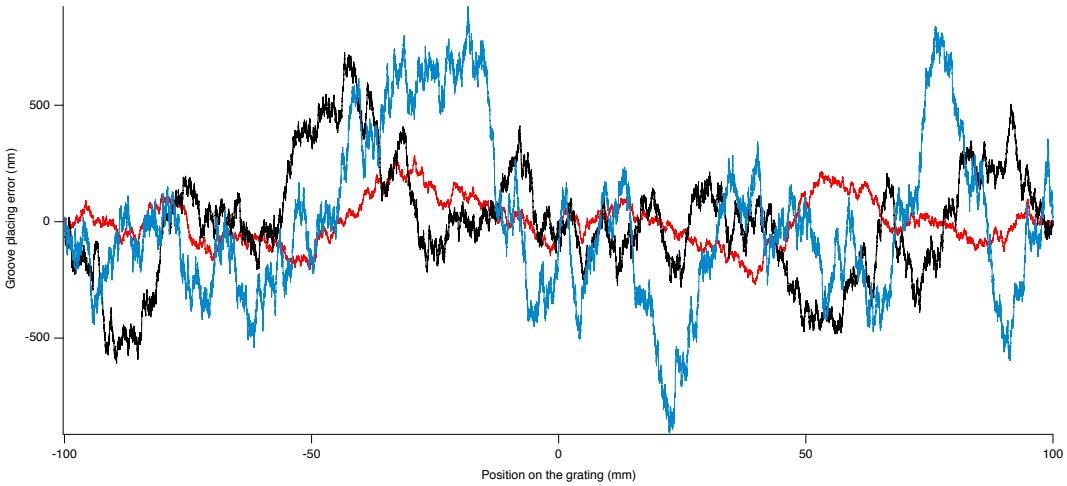

Figure 6: Three examples of the groove placing error curve used to simulate the effect shown in figure 5. The three curved represent a rms placing error of 99 nm (red curve), 240 nm (black curve) and 350 nm (blue curve). The curves represent the location of one particular groove with respect to its ideal position.

From the curves shown in figure 5, it is possible to extract both, the resolving power and the Strehl Ratio. From equations 10, one can calculate the SR for the given rms groove placing error. These values are reported in table 1.

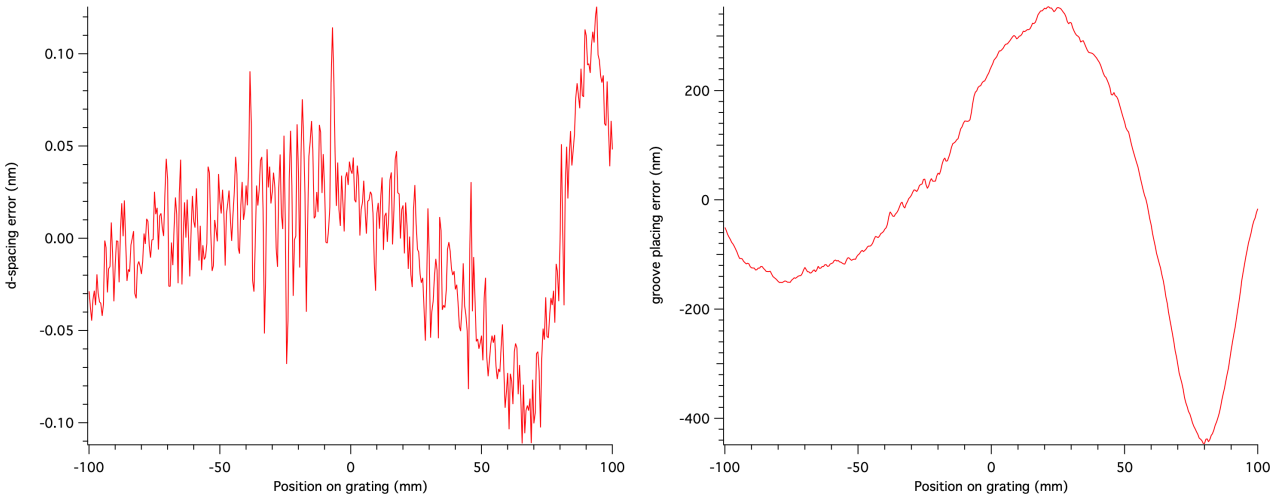

Figure 7: LEFT: Measured local pitch variation, extracted from the direct measurement of the local groove density and RIGHT: integrated value to estimate the groove placing error on the grating. The rms pitch error is < 0.1 nm rms. The overall groove placing error is 208 nm rms.

In the first column of table 1, the Normalized Resolving Power is also reported. This is the ration between the actual resolving power and the one obtainable with a perfect grating. In general, the target is to maintain the resolving power higher than 90% of its ideal value (e.g. with prefect optics) so, in this case, a placing error below 200 nm rms would have been desired. It is interesting to note that, the reduction in Resolving power is closer to the calculated SR than the measured SR. One cannot extract any definitive conclusion from this study, rather than this is a simple way to estimate the precision needed for the grating's groove placing precision without performing extensive and complicated simulations.

Table 1. Comparison of the Strehl Ratio extracted from figure 5 (3rd column) for various groove placing errors (first column) and the calculated SR using equation 10 (4th column). The simulated resolving power reduction for a give shape error is reported in the 2nd column.

rms placing error (nm)	**Normalized Resolving Power**	**Simulated SR**	**Calculated SR**
500 eV / 300 l/mm / using the generated groove placing error			
50	0.999	0.978	0.99
99	0.984	0.932	0.96
240	0.761	0.749	0.81
350	0.589	0.498	0.64
500 eV / 300 l/mm / using the measured groove placing error			
208	0.890	0.654	0.86

Note that, this is valid only if the beam is fully coherent or if the coherence length, as described in [38], of the beam is longer than the grating acceptance. For most of the standard SXR monochromator, when the number of illuminated lines is much higher than target resolving power, this assumption is not valid. This simple calculation should be applied to the length of a number of lines equal to the design resolving power

This work is partially performed under the auspices of the U.S. Department of Energy by LBNL under contract No. DE-AC02-05CH11231 and SLAC under contract No. DE-AC02-76SF00515.

The authors are grateful to May Ling Ng for the support during the measurement of the 300 l/mm grating and to Dmitriy Voronov, Howard Padmore and Antoine Wojdyla for the useful discussions.

REFERENCES

[1] B. Lai, F. Cerrina, SHADOW: A synchrotron radiation ray tracing program, Nucl. Instrum. and Meth. A, 246 (1986)
[2] K. Von Bieren, Pencil beam interferometer for aspheric optical surfaces, Proc. SPIE, 343 (1982) 101–108
[3] P.Z. Takacs, S.N. Qian, US patent No.U4884697, 1989.
[4] W. R. McKinney M. R. Howells, Design optimization of "straight groove" toroidal grating monochromators for synchrotron radiation, Nuclear Instruments and Methods, Volume 172 (1980)
[5] H. A. Padmore; Optimization of soft x-ray monochromators, Review of Scientific Instruments 60, 1608 (1989)
[6] R. L. Johnson, Grazing-incidence monochromators for synchrotron radiation Nuclear Instruments and Methods A Volume 246, (1986)
[7] Malcolm R. Howells, Plane grating monochromators for synchrotron radiation, Nuclear Instruments and Methods Volume 177, (1980)
[8] T. Harada and T. Kita, Mechanically ruled aberration-corrected concave gratings, Applied Optics Vol. 19, (1980)
[9] R. Reininger V.Saile, A soft X-ray grating monochromator for undulator radiation, Nuclear Instruments and Methods A Volume 288 (1990)
[10] C. T. Chen and F. Sette, Performance of the Dragon soft x-ray beamline, Rev. of Scientific Instrum. 60, 1616 (1989)
[11] H. Petersen, The plane grating and elliptical mirror: A new optical configuration for monochromators, Optics Communications Volume 40 (1982)
[12] R. Reininger, A.R.B. de Castro, High resolution, large spectral range, in variable-included-angle soft X-ray monochromators using a plane VLS grating, Nucl. Instrum. and Meth. A, 538, (2005) 760-770.
[13] D. Cocco, M. Marsi, M. Kiskinova, K.C. Prince, T. Schmidt, S. Heun, E. Bauer, Microfocusing VLS grating-based beamline for advanced microscopy. SPIE proc. Vol. 3767 p 271-279 (1999)
[14] R. Follath, The versatility of collimated plane grating monochromators, Nuclear Instruments and Methods in Physics Research A 467–468 (2001) 418–425
[15] G. Naletto and G. Tondello, A high resolution monochromator covering wide ultraviolet spectral ranges with a single grating, Pure and Applied Optics: Journal of the European Optical Society Part A, Volume 1, Number 6
[16] S. P. Hau-Riege, R. A. London, A. Graf, S. L. Baker, R. Soufli, R. Sobierajski, T. Burian, J. Chalupsky, L. Juha, J. Gaudin, J. Krzywinski, S. Moeller, M. Messerschmidt, J. Bozek, C. Bostedt, "Interaction of short x-ray pulses with low-Z x-ray optics materials at the LCLS free-electron laser," Optics Express 18, 23933-23938 (2010).
[17] L. Juha, V. Hajkova, J. Chalupsky, V. Vorlicek, A. Ritucci, A. Reale, P. Zuppella, M. Stoermer, Radiation damage to amorphous carbon thin films irradiated by multiple 46.9 nm laser shots below the single-shot damage threshold, J. Appl. Phys. 105, 093117 (2009).
[18] J. Krzywinski, D. Cocco, S. Moeller, and D. Ratner, Damage threshold of platinum coating used for optics for self-seeding of soft X-ray free electron laser, Opt. Express 23, 5397 (2015).
[19] J. Krzywinski, R. Conley, S. Moeller, G. Gwalt, F. Siewert, C. Waberski, T. Zeschke, D. Cocco, Damage thresholds for blaze diffraction gratings and grazing incidence optics at X-ray Free Electron Laser Journal of Synchrotron Radiation (2018), 25, 85-90
[20] E. Allaria, C. Callegari, D. Cocco, W.M. Fawley, M. Kiskinove, C. Masciovecchio, F. Parmigiani The FERMI@Elettra Free-Electron-Laser Source for Coherent X-Ray Physics ELETTRA Highlight 2010
[21] K. Yamauchi, H. Mimura, K. Inagaki, and Y. Mori, Figuring with subnanometer-level accuracy by numerically controlled elastic emission machining, Review of Scientific Instruments 73, 4028 (2002); https://doi.org/10.1063/1.1510573
[22] JTEC Corp. Japan, https://www.j-tec.co.jp

[23] S. Matsuyama, H. Nakamori, T. Goto, et al. Nearly diffraction-limited X-ray focusing with variable-numerical-aperture focusing optical system based on four deformable mirrors. Sci Rep. 2016;6:24801. Published 2016 Apr 21.
[24] D. Cocco, M. Idir, D. Morton, L. Raimondi, M. Zangrando, Advances in X-ray Optics: from metrology characterization to wavefront sensing-based optimization of active optics Nuclear Inst. and Methods in Physics Research, A, NIMA-D-17-01311 (2018)
[25] D. Cocco, Recent development in UV optics for ultra-short, ultra-intense coherent light sources Photonics 2015, 2(1), 40-49; doi:10.3390/photonics2010040
[26] Mahajan, Virendra, Strehl ratio for primary aberrations in terms of their aberration variance, J. Opt. Soc. Am., 73 (6): 860–861 (1983), doi:10.1364/JOSA.73.000860
[27] T. Pardini, D. Cocco, S. Hau-Riege Effect of slope errors on the performance of x-ray optics for X-ray free electron laser applications. Optics Express, vol. 23 – 25 pp 31889-31894 doi: 10.1364/OE.23.031889 (2016)
[28] L. Raimondi, D. Spiga, Mirrors for X-ray telescopes: Fresnel diffraction-based computation of point spread functions from metrology, Astron. Astrophys., 573 (2015) A22.
[29] L. Rebuffi, M. Sanchez del Rio, "OASYS (OrAnge SYnchrotron Suite): an open-source graphical environment for x-ray virtual experiments," Proc. SPIE 10388, 103880S (2017).
[30] M. Sanchez del Rio, L. Rebuffi, OASYS: A software for beamline simulations and synchrotron virtual experiments, AIP Conference Proceedings 2054, 060081 (2019)
[31] W.B. Peatman, Gratings, Mirrors and Slits, beamline Design for Soft-X-ray Synchrotron radiation Sources, Gordon and Breach Science Publishers, 1997.
[32] K.A. Goldberg, V.Y. Yashchuk, Optimized mirror shape tuning using beam weightings based on distance, angle of incidence, reflectivity, and power, Review of Scientific Instruments 87, 051805 (2016); doi: 10.1063/1.4950747
[33] F. Siewert, B. Löchel, J. Buchheim, F. Eggenstein, A. Firsov, G. Gwalt, O. Kutz, S. Lemke, B. Nelles, I. Rudolph, F. Schäfers, T. Seliger, F. Senf, A. Sokolov, C. Waberski, J. Wolf, T. Zeschke, I. Zizak, R. Follath, T. Arnold, F. Frost, F. Pietag and A. Erko, Gratings for synchrotron and FEL beamlines: a project for the manufacture of ultra-precise gratings at Helmholtz Zentrum Berlin, J. Synchrotron Rad. (2018). 25, 91-99
[34] S. Irick and W. R. McKinney, Measurement of diffraction gratings with a long trace profiler with application for synchrotron beamline gratings, AIP Conference Proceedings 417, 118 (1997); https://doi.org/10.1063/1.54581S.
[35] D. Cocco, G. Sostero, M. Zangrando, A technique for measuring the groove density of diffraction grating using the Long Trace Profiler Rev. Sci. Instr. Vol 74 (7) (2003) p. 3544
[36] S. Gleason, J. Manton, J. Sheaung, T. Byrum, C. Jensen, L. Jiang, J. Dvorak, I. Jarrige, P. Abbamonte, Intrinsic resolving power of XUV diffraction gratings measured with Fizeau Interferometer, Proceedings Volume 10385, Advances in Metrology for X-Ray and EUV Optics VII; 1038506 (2017)
[37] LCLS Strategic Facility Development Plan, https://lcls.slac.stanford.edu/sites/lcls.slac.stanford.edu/files/LCLS_Strategic_Development_Plan.pdf
[38] E. L. Church and P. Z. Takacs, "Specification of glancing-incidence and normal-incidence x-ray optics," Opt. Eng. 34, 353–360 (1995).